Thermography-inspired processing strategy applied on shearography towards nondestructive inspection of composites.

M. Kirkove*, Y. Zhao, P. Blain, J.-F. Vandenrijt, M. Georges

Centre Spatial de Liège, Université de Liège, Liege Science Park, B-4031 Angleur (Liège), Belgium

ABSTRACT

Shearography nondestructive inspection (NDI) based on the use of thermal stress in studied in view of detecting defects in composite materials. In particular, we would like to extract the content of information that is present in the deformation due to the evolving deformation during the variation of the stress. For that a good approach is to try to apply processing techniques which are largely applied in thermography NDI for the same purpose. We will discuss the necessity of pre-processing the shearography data to make them compatible with thermography inspired processing techniques. After that we will present the statistical analysis based on principal components, and we will discuss the possibility of deterministic analysis based on the temporal behavior during and after heating.

Keywords: Speckle interferometry, Nondestructive inspection, Fringe analysis

1 INTRODUCTION

Non-destructive inspection (NDI) techniques are used in order to detect damages in materials and structures. In particular, the composite materials used largely in the aeronautics industry yield an intensive research in finding the optimized NDI techniques to locate and quantitatively assess defect parameters. The most common NDI method is based on ultrasound [1] which requires direct contact with the inspected part or couplant, generally water in immersion tanks. Ultrasound testing usually measures in a single point and requires scanning. Among emerging methods, those based on imaging have the advantages of being contactless and full-field (no pointwise scanning required). In that category, one finds active thermography [2][3] and methods based on holography [4], in particular shearography [5]-[7]. Thermography is now a mature NDI method which is increasingly used in industries. Damage underneath the surface can be located through small surface temperature variations appearing when the sample undergoes some stress. A popular method for stressing the material is a brief thermal load from a flash lamp. Holography related methods allow visualizing the surface deformation due to the presence of underneath defects, which react differently than their surroundings to a given stress. Often thermography and holography (and related) are considered as complementary [8] and efforts to merge them provided interesting outcomes [9]-[11].

Shearography records the interference pattern between a speckle object wavefront and itself laterally displaced through an optical shearing device [5]. Such interference patterns, so-called shearograms, are recorded at different instants with different object stress conditions. The numerical difference between two shearograms gives rise to an intensity correlation pattern. For quantitative analysis, optical phase difference is often determined. Temporal phase-shifting permits to compute the phase of each recorded shearogram and the phase difference shows a phase map. In shearography, the latter is related to the derivative of the full-field displacement of the object under stress. The presence of a defect induces in the phase maps a specific local signature, which allows localizing the defect under the surface. The visibility of defects signatures depends on many factors like the material, the nature of the defect, its extent and depth. In a shearographic sequence, the defects appear at different instants depending on their depths. The detection of all the defects requires analyzing all the images of the sequence, which can be cumbersome and time-consuming. Efforts need thus to be carried out to ease the interpretation and more specifically, by the development of specific algorithms to automatically identify defects in a shearographic sequence [12][13].

*m.kirkove@uliege.be

Very few signal processing techniques have been developed for shearography. An automated defect detection algorithm based on the computation of the gradients of the phase maps was proposed in [13] and a technique based on principal component analysis (PCA) in [14]. In contrast, a broad variety of signal processing techniques have been developed for active thermography. The purpose of our work is to study the possibility of these approaches towards shearography by directly applying to shearographic data the most commonly used thermography processing (TP) techniques, a review of which is presented in [15].

Most of the TP techniques are applied in association to the optical pulse excitation method, where a brief intense heating is applied on the studied material. The temporal variation of temperature during the cooling shows the defects signatures appearing at different instants, mainly depending on the defect depth. Another stress method is to use modulated lamps (the so-called lock-in thermography) [16] but here we concentrate on the pulse heating. For the latter, some TP techniques analyze the statistical behavior in both and times: the principal component thermography (PCT) [17], the higher order statistics thermography (HOST) [18]. Other are deterministic: the differential absolute contrast (DAC) [19], the thermographic signal reconstruction (TSR) [20][21] and the pulsed phase thermography (PPT) [22], to name the most common ones. Sometimes they can be combined one another to take benefit of both: TSR and PPT [23], for instance. The last category allows retrieving the depth due to the fact that they aim at finding accurately the first appearance of defect, either by temporal or frequency analyses.

The work presented here deals with the application of TP to shearography image sequences showing evolution of deformation after heating. Unlike thermographic images sequences, shearographic phase map sequences do not show a monotonic behavior (wrapped phase map in both space and time). Generally, in shearography a well differentiated defect signature requires a longer heating (step heating) than what is necessary in thermography. Therefore, the possibility to apply TP must be addressed in view of this.

In this paper, we propose an optimized combination of pre-processing techniques for the shearographic data in order to be render possible the use of TP techniques, at least on the qualitative point of view. In section 2, we describe the test sample, the shearographic setup and the experimental data and present the processing strategy, divided in a pre-processing and processing steps. The pre-processing step is explained in section 3 and the processing step in section 4. In section 4, we present the statistical approach with the principal components analysis. In section 5, we discuss the analysis of some assumption for deterministic analysis based on the TSR. Section 6 concludes the paper.

2 SHEAROGRAPHY EXPERIMENT AND PROCESSING STRATEGY

2.1 Shearography experimental setup and data

The processing presented in this paper will be performed on phase maps temporal sequence obtained in a shearography NDI experiment on a sample with usual artificial defects used for investigating NDI methods. The sample consists of a monolithic plate of carbon fiber reinforced polymers (CFRP) which includes different types of artificial defects: flat bottom holes of circular shapes and Teflon inserts of triangular shapes. We already have studied the temporal behavior of these different types of artificial defects previously [24]. The area of the sample observed by the shearographic camera is shown in Figure 1(b). The defects positions, their shapes and their depths are precisely known; depth is reported in the figure.

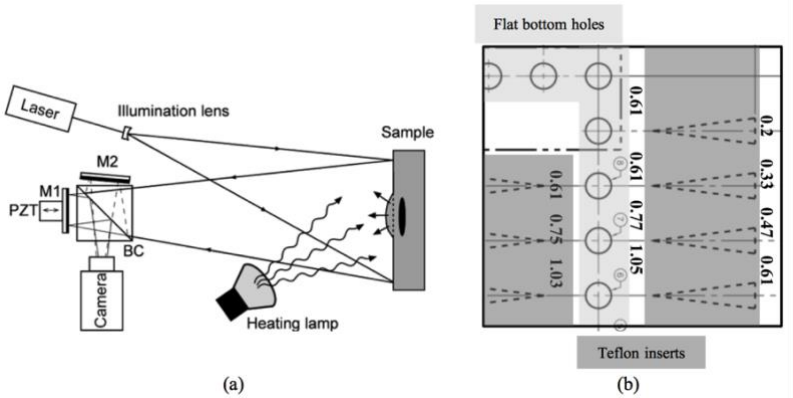

Figure 1 (a) Schematic of the shearography setup. (b) Area of the CFRP sample seen by the shearographic camera. Depths of some defects are indicated.

The shearography setup, the scheme of which is shown in Figure 1(a), is composed of a basic shearography head in a Michelson interferometer configuration. The image of the object illuminated by the laser is split in two equal images by a beam-splitter cube (BC). Both images travel to separate mirrors which reflect them to a CCD camera through the beam-splitter. One of the mirrors (M2) is slightly misaligned in order to produce a lateral displacement between both images (so-called shearing). At the overlap, interference occurs between the twin images, forming the so-called shearogram. A piezoelectric translator (PZT) placed on one of the mirror (M1) allows temporal phase-shifting for computing the phase of the recorded shearograms. Shearograms recorded at different instants during the heating allow computing phase difference between two states of the object. The thermal stimulus is produced by two 750 Watt halogen lamps. The laser illumination of the plate is performed by a 300 mW 532 nm DPSS laser the beam of which is extended by a lens. The plate is placed at about 1 meter from the lamps. A sequence of phase-shifted shearograms is acquired at the sampling frequency of 1 Hz.

Shearograms are recorded during before, during and after the step heating which lasts for a few seconds. The phase is computed for each of the shearogram by the phase-shifting. The shearogram before the heating starts is considered as the reference one, and it is subtracted from the phase obtained for all the subsequent ones. The result is phase difference (modulo 2π) which evolves during the heating and the cooling sequence. Figure 2 shows some phase maps taken out of the total sequence. At the beginning (Figure 2 (a)), the deformation starts, then some instants later, the flat bottom holes appear (Figure 2 (b)). When time increases during heating, the heat wave starts to deform other types of defects (the triangular Teflon inserts, Figure 2 (c)-(d)). The heating is stopped and the cooling sequence starts at t_c. The global deformation begins to decrease (less linear fringes) but the heat wave creates an increasing mechanical reaction to the Teflon inserts, while the flat bottom holes disappear, Figure 2 (f).

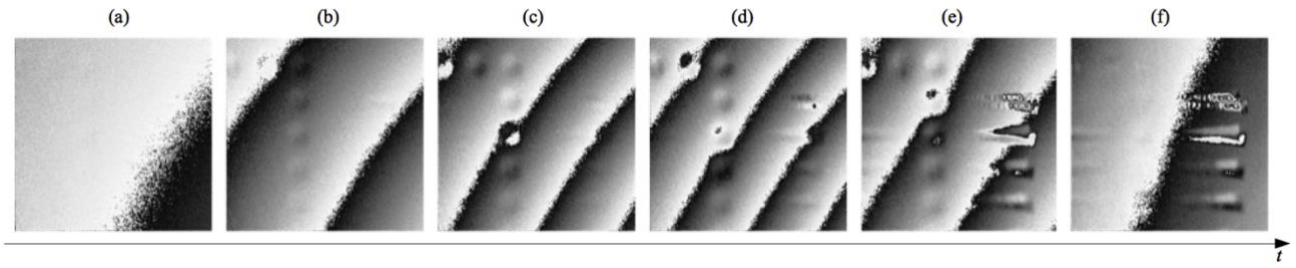

Figure 2 Temporal sequence of phase maps modulo 2π during and after step heating.

The purpose of this paper is to find a processing strategy applied on the basic data (phase of shearograms) in order to extract the images of defects of a typical sequence as it appears above.

2.2 Processing strategy for shearography inspired from thermography model

Figure 3(b) shows the block diagram of the proposed processing strategy that will be applied to shearography temporal data in a NDI experiment with a brief heat pulse. For a comparative purpose, Figure 3a shows the block diagram of the

standard thermography processing strategy. From the raw phase data of each shearogram, the processing chain should bring useful information on defects, whether quantitatively (deterministic approach) or qualitatively (statistical approach). For instance, the information can be parameters of defect (lateral extent, depth) or reduced set of images showing the defects, as is the case with the principal components analysis, for instance. The overall chain starts with a Pre-processing sub-chain, which will be described in section 3. Mainly it transforms the raw data (noisy phase modulo 2π) into a sequence of images with temporal monotonic behavior. After that, the main processing is the block *Adapted thermography processing* which can embody the adaptation of one of the TP techniques.

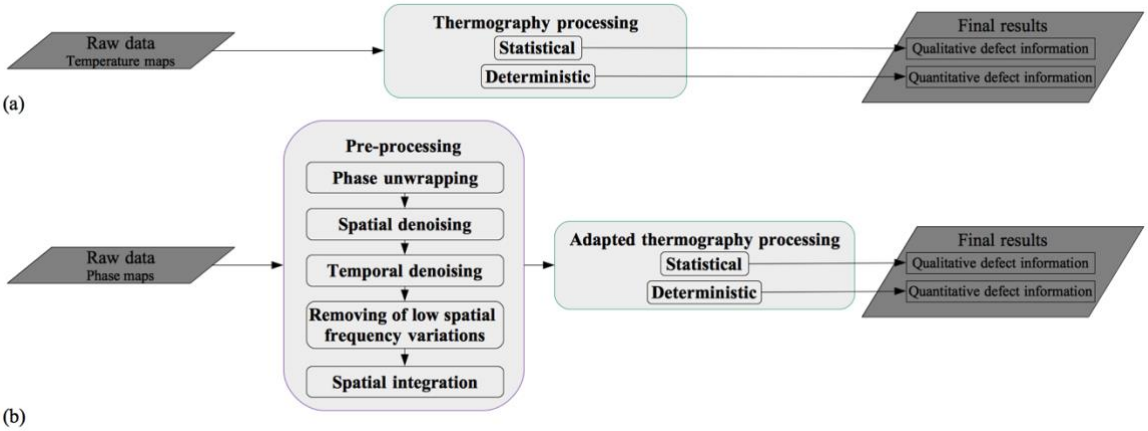

Figure 3 Block diagram of the proposed processing strategy (b) compared with thermography processing strategy (a).

3 PRE-PROCESSING

The first pre-processing step is ***phase unwrapping***. Indeed, shearography NDI produces phase maps at each instant t from subtraction of phase at instant t and phase at a given initial moment (reference state), for instance before heating has started, or at instant the temperature decay starts. Each spatial phase map shows phase modulo 2π values which are artifacts related to phase computation (result of arctangent function calculation). In order to eliminate such phase jumps, phase unwrapping can be applied following various strategies in interferometry [25]. Also, when considering a single pixel independently of its neighbors, the temporal values of phase is also obtained modulo 2π. In order to obtain monotonic data, temporal phase-unwrapping can be applied [26]. Temporal unwrapping has been performed on each pixel in our case. The result is an ensemble of spatio-temporal shearographic phase values. At any instant t in the series, phase image can be extracted and then spatially unwrapped.

We will see that the final step of pre-processing is integration. The latter can be strongly affected by noise in the initial image. Therefore, it is necessary to filter the unwrapped results. For that we apply two filtering stages. The first one is ***spatial denoising*** applied on each of the unwrapped phase maps at each instant t. It makes use of a non-linear median filter [27] that is more effective for preserving edges and reducing impulse noise compared to conventional linear filters [28][29]. The second stage is a ***temporal denoising*** applied on the spatially denoised sequence by considering the time responses at the pixels as different observations of a same phenomenon under different variables (here the pixels). The requirement of additional denoising after spatial denoising is justified as follows. The fourth pre-processing step (removing the low spatial frequency variations) applied after spatial denoising generates oscillations in the time responses at most pixels in the field. These degradations, due to the amplifications of the remaining noise, can affect the deterministic thermography processing techniques acting on the time responses. A time denoising is thus recommended just after spatial denoising for better preserving the regularity of the time responses. For that, PCA has been applied. In recent years, PCA has become a powerful tool for analyzing high dimensional data for data compression. In the PCA, the initial data set can be seen as a set of observations with respect to a set of variables. The PCA principle consists in converting the initial set of observations into a new set of variables called principal components (PCs), which are uncorrelated and ordered in such a way that the first ones contain most of the variation presented in all the original variables. The PCA filtering involves selecting some PCs, cancelling the others, forming the matrix of the so modified PCs and inverting the initial decomposition. Reference [30] describes the state-of-the-art methods for selecting the number of non-zero PCs. Among these methods, we have chosen one of the most popular criteria based on the cumulative percentage of total variation. With this criterion, only three PCs are selected and the higher PCs were left off

in the reconstruction of the temporal phase value in each pixel. In order to apply PCA, the 3D matrix representing the sequence of images should be rearranged into a 2D one. The pixels ensemble consists of a set of spatial variables which can be rearranged on a single line with length $N_s = N_x$ x N_y, while the value of each pixel is arranged in a column with length N_t. This gives rise to a 2D matrix X with space in one direction and time in the other. The standard implementation of the PCA decomposition consists of the diagonalization of the covariance matrix of the initial matrix (XX^T) [31]. Since its dimension (N_s x N_s) is generally too huge, its diagonalization encounters computational problems. To circumvent these problems, the PCA decomposition is made, as in [32], using singular value decomposition (SVD) and only keeping the first N_t eigenvalues from the N_s ones.

A further pre-processing consists in ***removing the low spatial frequency variations*** by a polynomial correction. This step is mandatory in the case of interferometric methods. The latter are strongly sensitive in any phase variation. When observing a temporal sequence of interferograms, such as shown in Figure 2, spurious global phase shifts may appear in some of the images of the sequence. Such phase variation can be due to sudden mechanical or environmental disturbances in the laboratory. While this does not affect the capture of the shearograms, the spurious phase needs to be removed prior to processing. This technique consists in applying a polynomial regression to each image and subtracting the result from it. From the corrected sequence, the last pre-processing stage can be applied.

The last pre-processing is ***spatial integration***. It is necessary because in shearography the defect signatures consist of two lobes in the phase difference, with opposite signs between both. Therefore, it can be difficult to perform a quantitative assessment using the TP methods. For that it would be more appropriate to work directly with deformation sequence (as obtained with ESPI) than on sequence of deformation derivatives (as here in shearography). The integration is performed on each spatial phase map at a time, and the final result will be used in the processing. The integration of a shearographic image is realized using a solution of an inverse problem. A key element in inverse problem resolution is to have an appropriate mathematical expression for the forward model, i.e., the model relating the observations to the original data. In the current context, the forward model, relates the phase $\Delta\phi_s$ measured by shearography and $\Delta\phi_e$ the actual phase related to the deformation (i.e. as is measured by ESPI). By defining Δ_s the displacement operator in the shear-direction as the operator mapping the image $\Delta\phi_e$ on the image defined at coordinates (x, y) by $\partial\Delta\phi_e(x,y)/\partial s$, the forward model can be rewritten as

$$\Delta\phi_s(x,y) = (\Delta_s(\Delta\phi_e))(x,y) + n_s(x,y), \tag{1}$$

where n_s is an additive noise. After rearranging the images $\Delta\phi_e$, $\Delta\phi_s$, and n_s as linear vectors f, g and n, this equation can be rewritten in the following more general form

$$g = Af + n, \tag{2}$$

where A is the matrix representing a convolution. The alternating direction method of multipliers (ADMM), originally proposed in [33], emerged recently as an efficient optimization approach for several inverse problems, in particular, deconvolution problems such as (2) where n is a white Gaussian noise. ADMM-based approaches employ priors/regularizers, such as those based on wavelets or total variation (TV) [34]. In the model (2), the pixels located near the boundary of the observed image (g) depend on pixels of the original image (f) outside of its domain. The typical way to formalize this issue is to adopt a periodic boundary condition that is unnatural and produces ringing artefact emanating from the boundaries [35]. Assuming that the boundaries are unknown is a more realistic assumption. In that case, the vector f in equation (2) contains more samples than g since it includes the boundary ones and the vector g is obtained by selecting the indices of samples that do not depend on boundary pixels. If we indicate by M the masking matrix performing this operation, assuming unknown boundaries permits to rewritten equation (2) as

$$g = MAf + n, \tag{3}$$

In [35], the ADMM-based approach for image deconvolution is extended under assumption of unknown boundaries, i.e. for solving image deconvolution problems such as (3) via the resolution of the following minimization:

$$\underset{f}{\operatorname{argmin}}\left(\frac{1}{2}\|g - MAf\|_2^2 + \alpha\phi(f)\right), \tag{4}$$

where $\|\ \|_2$ is the l_2-norm defined as $\|x\|_2 = \sum_{i=1}^{N} |x_i|^2$ for $x \in \mathbb{R}^N$, ϕ is a regularizer and α is a regularization parameter. Two standard regularizers are proposed in [35]: wavelet- and TV- based. We cannot use the TV-based regularizers to inverse problems where the convolution operator is a displacement operator. Indeed, TV-based regularizers assume that the convolution operator applied to the vector with all components sets at 1 differs from the null vector and the displacement operator does not fulfill this assumption. For the wavelet-based regularizers, four algorithms

have been proposed in [35]: the FA-MD, FA-CG, FS-MD and FS-CG algorithms. We have chosen the FA-MD algorithm that outperform the others in terms of convergence speed and improvement in signal-to-noise ratio. In FA-MD, the regularizer is expressed as $\phi(x) = \|P(x)\|_1$ where P is the matrix of wavelet decomposition and $\|\ \ \|_1$ is the l_1-norm defined as $\|x\|_1 = \sum_{i=1}^{N} |x_i|$ for $x \in \mathbb{R}^N$.

Figure 4a-e shows the result after applying the pre-processing chain described above. We have considered a given instant in the whole sequence which contains 163 images where both the circular flat bottom holes and the triangular Teflon inserts are visible. Nevertheless, the effect of pre-processing is equivalent on every image of the entire sequence. Figure 4f-j shows the time responses at a given pixel. It was chosen in the negative lobe of one of the circular flat bottom holes. We see that, before integration (Figure 4f-i), the relative phase decreases during the heating and increases after the heating is stopped. This is because the negative lobe of the derivative has an inverted sign compared to the true deformation which is positive (as is intuitively understandable in such experiment). The sign of the corresponding positive lobe has, obviously a positive increase in phase during the heating before integration (not shown).

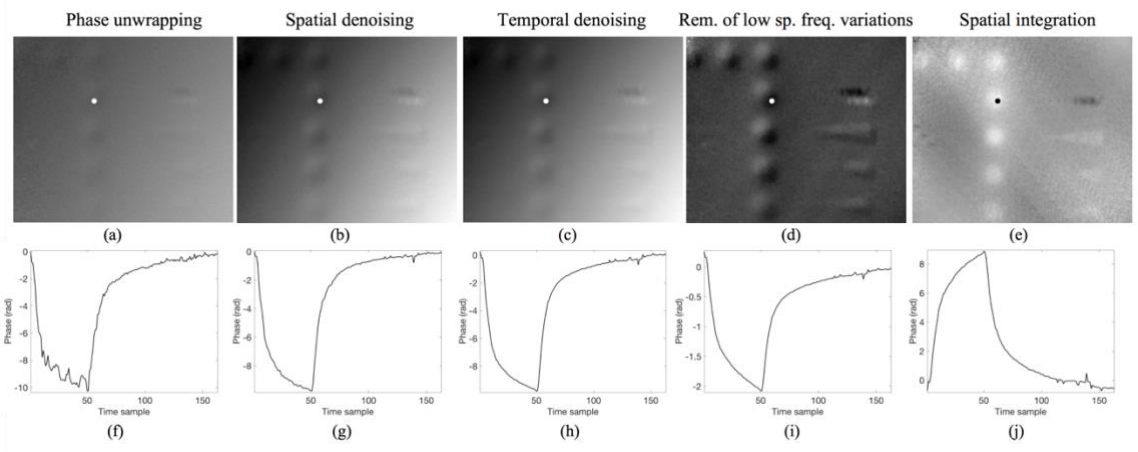

Figure 4. Proposed pre-processing combination: phase maps at the 20th instant (a-e) and time responses at a given pixel in a negative lobe of one of the circular flat bottom holes (f-j). The dot indicates the position of the given pixel.

Concerning the spatial denoising by median filtering, the effect can be easily noticed on the image, but it is surprisingly effective on the temporal behavior as well. The temporal denoising has not only smoothing effect on the time as expected but also a very positive influence in the contrast of the image. The polynomial correction effect is more distinct to see in the image since it is directly applied on every image. On the final integrated result, we obviously see that now all defects that the local defect signature (local deformation) has the shape of the artificial defect and is only positive or negative. We observe that an artefact in the form of diagonal trails has appeared during the integration process. The diagonal trails follow exactly the direction of the shear used experimentally and result from integration of the residual noise remaining after previous pre-processings. The sign of the temporal behavior has been inverted after the integration compared to previous curves.

Figure 5 gives the phase images at different instants of the pre-processed sequence. This sequence has been used as input of the processing step described in the following section.

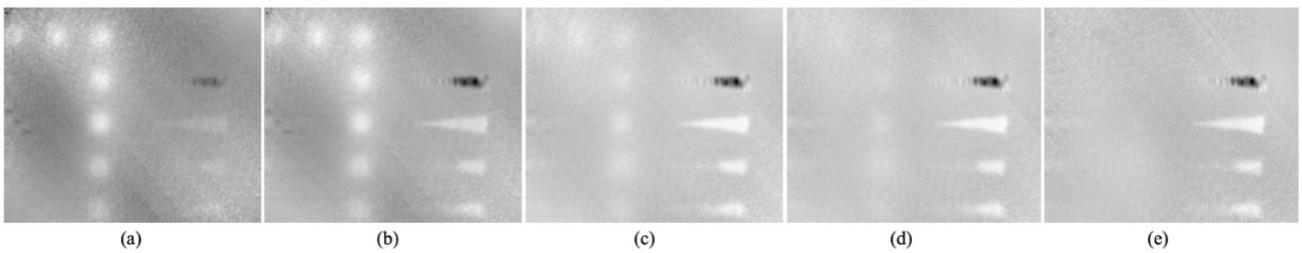

Figure 5. Phase images at instants 20, 50, 60, 70, 120 of the pre-processed sequence.

4 PROCESSING BY THE STATISTICAL APPROACH

4.1.1 Principal Components Thermography (PCT) model

The PCT technique consists on applying PCA on a set of thermograms time series. Then, the calculated eigenvalues are ranked by decreasing values and the corresponding eigenvectors are ranked accordingly. In that way, the first eigenvectors contain the most variance of the sequence. Usually, a set of thermograms can be adequately represented with only a few eigenvectors, *e.g.* 10 or less [15]. The first eigenvector is generally a homogeneous image of no interest since it contains the main temperature elevation undergone by the sample. The next eigenvectors (2 or 3) often show defects which have generated a higher spatio-temporal variation in the sequence. The highest order eigenvectors gradually become very noisy.

As for PCA filtering (see section 3), the application of PCA on a sequence of images assumes that a sequence is represented with a 2D matrix X of dimension N_s x N_t, where N_s is the size of the space dimension and N_t the size of the time dimension. The standard implementation of the PCA decomposition consists of the diagonalization of the covariance matrix of the initial matrix (XX^T) [31]. Since its dimension (N_s x N_s) is generally too huge, its diagonalization encounters computational problems. To circumvent these problems, instead of computing the covariance of X, we rather compute the covariance matrix of its transpose matrix X^T (X^TX), which has a much lower dimension (N_t x N_t). Then, we obtain the eigenvectors of XX^T by left multiplication of the eigenvectors of X^TX by X.

While the PCT is often applied in the case of pulse heating, using thermograms sequence after the pulse, this is not a prerequisite. Indeed, it is sufficient that sufficient spatio-temporal variations are observed in the signal to make such statistical analysis useful. For instance, it can work with other types of excitation such as heating applied on longer time, e.g. by step heating.

4.1.2 Application to shearography data - Principal Components Shearography (PCS)

In shearography we have applied the PCA on the 163 images which were previously pre-processed (Figure 5). The result is shown in Figure 6, which displays the five first eigenvectors, from Figure 6(a) to Figure 6(e). We can see that only the two first eigenvectors show the defects, while the three last ones contain mainly noise. This shows the effectiveness of the PCA for data reduction, where 163 images are efficiently reduced to only two of interest. The other ones show the artifact due to the integration process. These oblique lines can be observed in the integration result, at the end of the pre-processing (Figure 5).

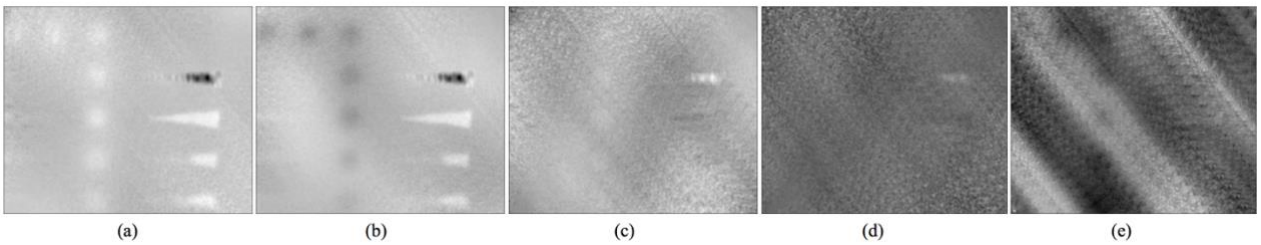

Figure 6. Results of PCS: (a)-(e) show respectively eigenvector 1 to 5.

In PCT, as already discussed before, the first eigenvector does not generally show the defects but rather the main temperature elevation (low spatial frequency). Often the eigenvectors of interest are the second and the third ones. In PCS results shown here, the two first eigenvectors are of interest. The result of PCA strongly depends on the initial data, thus the exact number of useful eigenvectors could be different. However, the tendency discussed here is still valid.

5 PROCESSING BY THE DETERMINISTIC APPROACH

In thermography, the surface temperature at each pixel varies monotonically in time. A large number of thermography NDI are based on the use of pulse or flash lamps, often referred as optical pulse thermography (OPT). Such stress method consists to shine the sample with a brief intense heating provided by a flash lamp. After the heat pulse, the sample temperature is decreasing. During the cooling period, the time responses of thermographic data at non-defective pixels follow the decay curve given by the one-dimensional approximate solution of the heat diffusion equation [15] which is inversely proportional to $\sqrt{t}$, with t the time during the cooling period, starting at some instant t_c.

An efficient deterministic approach to post-process thermography data is the thermographic signal reconstruction (TSR) [20][21][36][37]. It consists of fitting the experimental temperature data to the heat diffusion equation, more specifically a polynomial fit of its logarithmic version given hereafter

$$\ln(T(t)) = \ln\left(\frac{Q}{e}\right) - \frac{1}{2}\ln(\pi t), \quad (5)$$

where $T(t)$ is the temperature profile, Q is the input energy and e is the thermal effusivity. Polynomial fit of Eq. (5) can easily show defects signature first appearance through coefficients of fit which appear different at defects than for their neighborhood. Defect depths can be estimated from such analysis. Other methods are based on the frequency analysis of the temporal temperature decay after t_c. The most popular one is the pulse phase thermography (PPT) [22]. These methods also assume a similar temporal behavior. Various frequencies can be retrieved showing the defects at various depths, a given depth being associated with a given frequency.

In the following we discuss the possibility of such deterministic approach applied to a temporal series of shearographic interferograms. The question of the applicability of TP methods must be clearly addressed in regards of the thermal excitation. The relationship between the deformation and the temperature variation is given by the thermal expansion coefficient, which sets the sensitivity of interferometry methods for detecting defects through heating with lamps.

From the experiments we have carried out, the usual flash lamps used in thermography (a few kJoules emitted on a few milliseconds) do not allow to provoke sufficient stress to observe many defects, as compared with thermography. Instead continuous halogen lamps are used in the step heating way, which allow heating the sample for a few seconds. During heating the sample deformation increases. Often, shearography operators observe what happens in the cooling (i.e. when the deformation is decreasing). So a question arises: is it possible to apply the deterministic TP to retrieve information on the defect, mainly its depth (or at least provide indication of the latter)?

This would be the ideal case of a sudden high deformation, followed by analysis of phase during the relaxation. Such an ideal case would require flash lamps which much higher energy than the current one we used so far. If such possibility is offered, we have to be cautious that the deformation relaxation follows a similar decrease than its temperature counterpart in thermography; hence its logarithm $\ln(\Delta\phi_e(x, y, t))$ is linear.

From the preprocessed series of phase maps, we need finding the moment of change, which in fact corresponds to the starting of cooling time t_c in thermography, where t_c is generally considered as an invariant constant at each pixel. However, we don't know a priori if this situation is the same in shearography, during the mechanical relaxation. To assess it, we compute the index of the last saturated response at each pixel as the maximum of the time indices with values larger than a threshold. This threshold is pixel-dependent: it is the maximum of the time response minus a percentage of the width of the time response range. The returned index incremented by 1 provides t_c. The procedure repeated for each pixel provides a t_c map.

We need to assess that the time responses have a quasi-linear behavior in the logarithmic domain inside their cooling period. To that purpose, we apply a quadratic polynomial regression to the part of each time response from its t_c value. We compute the coefficient of determination (R^2)which serves as an indicator of the quality of the regression. The quasi-linear behavior at one pixel is validated if its R^2-value is greater or equal to a threshold, *e.g.* 0.9. The procedure is repeated for each pixel to provide a thresholded R^2 map.

A representation of the distribution of the t_c-values is obtained by its histogram shown in Figure 7(a) (upper part, with zoom at lower part). It shows that 92.9% of the pixels have their t_c values in the range [52, 55]. The purple area in Figure 7(b) shows the zone where the t_c values are “abnormal” (not in the tight range [52, 55]). We see that these pixels are almost located in non-defective areas where the integration artifact is important. The green area in Figure 7(c) shows the zone where the R^2 values of the linear fit are below the threshold 0.9, where thus the quasi-linear behavior is not validated. The ratio of the pixels in the green area with respect to the entire image is 93.6%. The blue values show all the invalid pixels found by both previous approaches, Figure 7(d). We see that the invalid pixels are almost all in non-defective areas where the artefact is important, only a few part in the triangular defective areas, mainly on the shallower defect on the top.

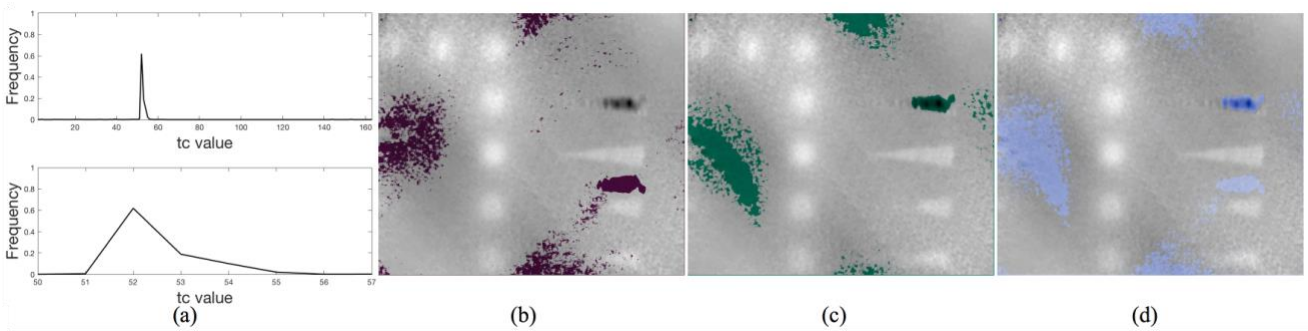

Figure 7. Validation of linear behavior of the logarithm of the phase during relaxation. (a) histogram of t_c-values,(b) t_c map with invalid pixels in purple (out of the range [52,55]), (c) R^2 map (invalid in green) and (d) both maps (invalid in blue). All the maps are superimposed on the 20th image of the pre-processed sequence.

So far, we can conclude that the deterministic approaches could be valid in shearography when dealing with the relaxation. Yet there remains the question of the practical applicability of a very strong and brief thermal stress.

In the more usual case of the step heating, we see that the defect signatures already appear during the heating. Therefore, one should look at the temporal signal of $\Delta\phi_e(x,y,t)$ or $\ln(\Delta\phi_e(x,y,t))$ in order to retrieve map of defects in function of time. However, quantitative assessment would require some analytical or simulated modeling to allow extraction of depth from specific instants retrieved from the sequence.

6 CONCLUSION

In the paper, we have shown the processing of shearographic sequence obtained on a composite sample with artificial defects and stressed by step heating of a halogen lamp. The defects appear at different moments in function of their depth. In a similar way to what is done in thermographic NDI, we wanted to process the full temporal series in order to extract the rich content of such data series to improve qualitatively the detection of defects, and possibly obtaining a quantitative information about defect depth. Inspired by such thermography processing methods, we studied their implementation to shearography. First we found that we need to preprocess shearographic data in order to render them monolithically in time, like thermograms. Also various filtering needed to be performed prior to the last pre-processing which is spatial integration, which otherwise is affected by noise. Once pre-processed, the data series can be processed by two types of approaches. The first one is based on the statistical analysis of shearograms series. In particular, the principal components shearography (PCS) is useful for qualitative purpose. Like its widely used thermography counterpart (PCT), PCS allows to retrieve a set of two images containing all defects, out of a series of a few hundred initial images. To go deeper, for quantitative assessment of defect parameter like depth, deterministic approaches have to be followed. In particular, in thermography, the temporal behavior after brief heating is known through solution of the heat diffusion equation. From this, one can apply temporal fitting methods, like TSR, or other based on frequency analysis, like PPT. Applying this in shearography requires that temporal evolution follows the same law than in thermography which was verified. However, this is not sufficient because the stress must be brief and intense to generate a sudden deformation and analyze the latter with methods equivalent to TSR or PPT. Such excitation means was not considered so far. Instead, the step heating allows stressing sufficiently the samples to allow observation of defects. However, the excitation is much slower (a few seconds) and the defects signatures already appear during the heating. Therefore, we would need to analyze what happens during heating and develop models to extract the defect parameters from this part of the object response.

ACKNOWLEDGMENTS

The study presented in this work has been achieved with financial support of Wallonia under the project TECCOMA (contract 7281) in the frame of SKYWIN competitiveness pole.

REFERENCES

[1] Blitz, J. and Simpson, G., [Ultrasonic Methods for Non-Destructive Testing], Chapman & Hall (1992)
[2] Maldague, X., [Theory and Practice of Infrared Technology for Nondestructive Testing], Wiley-Interscience (2001).

[3] Jorge, I., Venegas, P., Vega, L., Lopez, I., Vollheim, B., Krausz, L., and Georges, M., “Review of thermal imaging systems in composite defect detection,” Infrared Physics & Technology 61, 167-175 (2013)
[4] Kreis, T., [Handbook of Holographic Interferometry: Optical and Digital Methods], Wiley-VCH Verlag GmbH | Co. KGaA, Weinheim (2005)
[5] Steinchen, W., Yang, L., [Digital Shearography: Theory and application of digital speckle pattern shearing interferometry], SPIE Press, Bellingham (2003)
[6] Kalms, M., and Osten, W., “Mobile shearography system for the inspection of aircraft and automotive components, ” Opt. Eng. 42 (5), 1188- 1196 (2003)
[7] Viotti, M., Albertazzi, A., [Robust Speckle Metrology: Techniques for Stress Analysis and NDT], SPIE Press, Bellingham (2014)
[8] Georges, M.P., “Comparison between thermographic and holographic techniques for nondestructive testing of composites: similarities, differences and potential cross-fertilization,” Proc. SPIE 9660, 966002 (2015)
[9] Georges, M. P., Vandenrijt, J.-F., Thizy, C., Alexeenko, I., Pedrini, G., Rochet, J., Vollheim, B., Lopez, I., Jorge, I., Rochet, J., and Osten, W., “Combined holography and thermography in a single sensor through image-plane holography at thermal infrared wavelengths,” Opt. Exp. 22, 25517-25529 (2014)
[10] Georges, M. P., “Speckle interferometry in the long-wave infrared for combining holography and thermography in a single sensor: applications to nondestructive testing: The FANTOM Project,” Proc. SPIE 9525, 952557 (2015).
[11] Georges, M.P., “Long-wave infrared digital holography,” in New Techniques in Digital Holography (ed. P. Picart), John Wiley & Sons, Inc., pp. 219-254, Hoboken, NJ, USA (2015)
[12] Fantin, A. V., Willemann, D. P., Viotti, M., and Albertazzi, A, “A computational tool to highlight anomalies on shearographic images in optical flaw detection,” Proc SPIE 8788, 87880L (2013)
[13] Vandenrijt, J-F., and Georges, M., “Automated Defect Detection Algorithm Applied to Shearography in Composites,” in *Fringe 2013*, 2014, pp. 237–240.
[14] Vandenrijt, J-F., Lièvre, N., and Georges, M., “Improvement of defect detection in shearography by using principal component analysis,” Proc SPIE 9203, 92030L (2014)
[15] Ibarra-Castanedo, C., Avdelidis, N. P., Grenier, M., Maldague, X., and Bendada, A., “Active thermography signal processing techniques for defect detection and characterization on composite materials,” Proc. SPIE 7661, 76610O (2010).
[16] Busse, G., Wu, D., Karpen, W., "Thermal wave imaging with phase sensitive modulated thermography," J. Appl. Phys. 71(8), 3962-3965 (1992)
[17] Rajic, N., “Principal component thermography for flaw contrast enhancement and flaw depth characterization in composite structures,” Compos. Struct. 58(4), 521–528 (2002).
[18] Madruga, F. J., Ibarra-Castanedo, C., Conde, O. M., Maldague, X. P., and López-Higuera, J. M., “Enhanced contrast detection of subsurface defects by pulsed infrared thermography based on the fourth order statistic moment, kurtosis,” Proc. SPIE 7299, 72990U (2009)
[19] Pilla, M., Klein, M., Maldague, X. & Salerno, A., "New absolute contrast for pulsed thermography," in Proc. Quantitative Infrared Thermography 5, Dubrovnik, Croatia, 53-58 (2002)
[20] Shepard, S., Lhota, J., Rubadeux, B., Wang, D., Ahmed, T., "Reconstruction and enhancement of active thermographic image sequence," Opt. Eng. 42(5), 1337-1342 (2003)
[21] Shepard, S., "Flash thermography for aerospace composites," IV Conf. Panamericana de END, Buenos Aires, Oct 2007, available online on https://www.ndt.net/article/panndt2007/papers/132.pdf
[22] Ibarra-Castanedo, C., Maldague, X. P., “Review of pulsed phase thermography," Proc. SPIE 9485, 94850T (2015)
[23] Ibarra-Castanedo, C., Piau, J-M., Guilbert, S., Avdelidis, N., Genest, M., Bendada, A., Maldague, X., “Comparative study of active thermography techniques for the nondestructive evaluation of honeycomb structures," Res. NDE 20 (1), 1-31 (2009)
[24] Blain, P., Vandenrijt, J-F., Languy, F., Kirkove, M., Theroux, L-D., Lewandowski, J., and Georges, M., “Artificial defects in CFRP composite structure for thermography and shearography nondestructive inspection,” Proc. SPIE 10449, 104493H (2017)
[25] Ghiglia, D., and. Pritt, M.D, [Two-Dimensional Phase Unwrapping: Theory, Algorithms, and Software], Wiley, (1998).
[26] Huntley, J., and Saldner, H., “Temporal phase-unwrapping algorithm for automated interferogram analysis,” Appl. Opt. 32 (17), 3047–3052 (1993).
[27] Bose, T., [Digital Signal and Image Processing]. John Wiley & Sons, Inc.(2003)

[28] Pitas, I., and Venetsanopoulos, A., [Nonlinear Digital Filters: Principles and Application]. Kluwer Academic Publisher (1990).
[29] Bovik, A. C., Huang, T. S., and Munson, J. D. C., "The Effect of Median Filtering on Edge Estimation and Detection," IEEE Trans Pattern Anal Mach Intell, 9 (2), 181–194 (1987).
[30] Karlis D., Saporta G., and Spinakis A., "A simple rule for the selection of principal components," Communications in Statistics - Theory and Methods, 32(3), 643–666, (2003).
[31] Shlens J., "A tutorial on principal component analysis," 2003.
[32] Rajic N., "Principal component thermography for flaw contrast enhancement and flaw depth characterisation in composite structures," Composite Structures, 58(4), 521–528, (2002).
[33] Gabay D., Mercier B., "A dual algorithm for the solution of nonlinear variational problems via finite element approximation", Computers and Mathematics with Applications, 2(1), 17-40, (1976)
[34] Alfonso M. V., Bioucas-Dias J. M., Figueiredo M. A. T., "An augmented Lagrangian approach to linear inverse problems with compound regularization", *IEEE International Conference on Image Processing*, Hong Kong, 4169–4172 (2010).
[35] Almeida, M. S. C., and Figueiredo, M., "Deconvolving images with unknown boundaries using the alternating direction method of multipliers," *IEEE Trans. Image Process.*, 22 (8), 3074–3086 (2013).
[36] Balageas, D. L., Roche J.-M., Leroy F.-H., Liu W.-M., Gorbach A. M., "The thermographic signal reconstruction method: A powerful tool for enhancement of transient thermographic images," *Biocybernetics and Biomedical Engineering*, 35 (1), 1–9 (2015).
[37] Roche J.-M., Leroy F.-H., Balageas, D. L., "Images of TSR coefficients: a simple way for rapid and efficient detection of defects," *Materials Evaluation*, 72(1), 73–82 (2014).